# Method for Estimation of Electrical Distance Between Antennas Based on MUSIC-Type Algorithm

Nikola Basta and Miljko Erić

***Abstract*—A method for estimation of electrical distance between two realistic antennas, based on a MUSIC-type algorithm, is proposed. A simple physical model of the antennas is assembled in a full-wave electromagnetic simulation tool. The synthesized signal accounts for the transfer function between antenna ports, which is extracted from the electromagnetic simulation. The method is verified through comparison with the actual distance within the electromagnetic model and with the computed normalized group-delay.**

***Index Terms*—distance measurement; radio positioning; ToA estimation; MUSIC algorithm;**

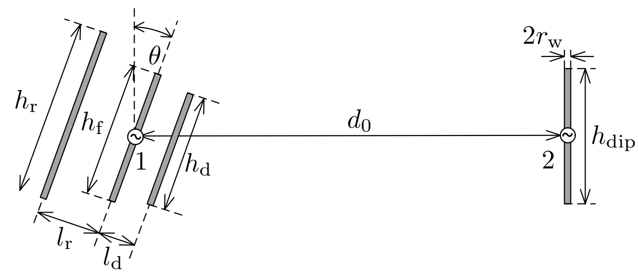


Fig. 1. Half-wave dipole and Yagi-Uda antenna, placed at distance $d_0$ in the simulated two-antenna scenario.

## I. Introduction

DEVELOPOMENT of the global navigation satellite systems (GNSS) and the increase of processing power of the handheld devices was immediately followed by development of indoor positioning systems. Indoor positioning, as well as GNSS, found their way to many commercial, military and safety-of-life applications. In the heart of all positioning algorithms lies the measurement of distance between the transmitter and the receiver, using the information on the signal power, phase or time of arrival (ToA) [1], [2]. The radio ranging algorithms that are based on observation of the time of arrival (ToA) of the signal, actually estimate *electrical* [3] rather than physical distance between the transmitter and receiver antennas. The antennas are often roughly approximated by point radiators, which do not account for propagation of the signal within the antennas themselves. The consequence of this mismodeling is performance degradation of ranging, localization and direction-of-arrival (DoA) estimators. The information on the propagation of the electrical signal in the antennas is carried within the frequency- and angle-dependent phase and group-delay characteristics of the transfer function between the antenna ports [2], [4], [5]. In many cases, this transfer function cannot be measured *in situ*. Since there is a constant demand for high-level positioning accuracy, it is important to revisit the problem of estimation of electrical distance with a careful modeling of the received signal.

In this work we elaborate the signal model and propose a MUSIC-type algorithm [6]–[8] for estimation of electrical distance between two antennas in a typical narrowband ranging procedure. In order to assess the error contribution of the ranging algorithm, we compare the estimates to the normalized group delay, derived from the transfer function between the antenna ports that is obtained from an electromagnetic simulation of the scenario.

Nikola Basta is with the School of Electrical Engineering, University of Belgrade, 73 Bulevar kralja Aleksandra, 11120 Belgrade, Serbia (e-mail: nbasta@etf.rs).

Miljko Erić is with the School of Electrical Engineering, University of Belgrade, 73 Bulevar kralja Aleksandra, 11120 Belgrade, Serbia (e-mail: meric@etf.rs)

## II. Problem formulation

We consider a system consisting of a transmitter and a receiver antenna, set apart by physical distance $d_0$ (Fig. 1). The position of each of the antennas is determined by a fixed point at or close to the geometrical center of the antenna in question. The signal that is being transmitted is a periodic sequence of $N$ symbols and of bandwidth $BW$, modulated at central frequency $f_{\mathrm{c}}$. It is assumed that the transmitter and the receiver have perfectly synchronized reference clocks. The problem in focus is estimation of the electrical distance between the antenna ports for different orientations of the transmitting antenna and different sequence lengths $N$. The estimation is based on $M$ transmitted frames of the *a priori* known signal sequence.

## III. Electromagnetic simulation setup

The setup for the electromagnetic simulation consists of a transmitting three-element Yagi-Uda antenna (port 1) and a receiving half-wave dipole antenna (port 2), placed in vacuum at distance $d_0 = 5\,\mathrm{m}$, as shown in Fig. 1. The antennas are realized as wire models in a full-wave solver WIPL-D Pro [9]. They are optimized for operation at central frequency $f_{\mathrm{c}} = 1\,\mathrm{GHz}$, from which the central free-space wavelength follows, $\lambda_{\mathrm{c}} = c/f_{\mathrm{c}} \approx 0.3\,\mathrm{m}$. The radius of the model wires is $r_{\mathrm{w}} = \lambda_{\mathrm{c}}/100$. The Yagi-Uda antenna is inclined by angle $\theta$ and is defined by the lengths of the reflector, feeder and

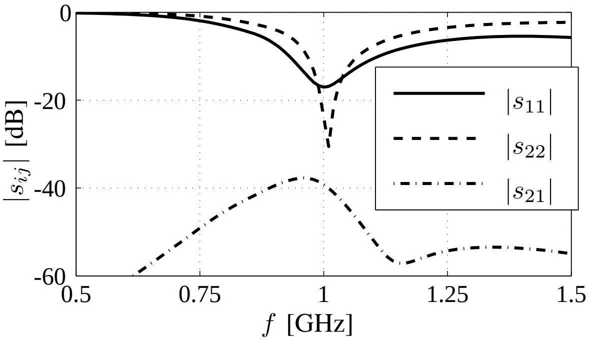


Fig. 2. Scattering parameters of the two antennas for $\theta = 0°$.

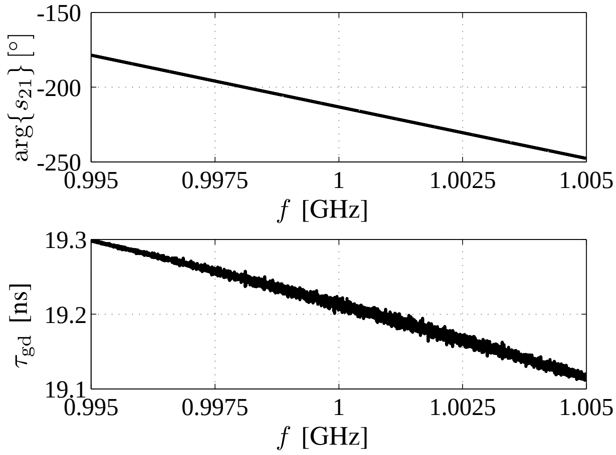


Fig. 3. Phase and group delay of the transmission parameter $s_{21}$ vs. frequency for $\theta = 0°$.

director elements, respectively: $h_{\mathrm{r}} = 0.5\lambda_{\mathrm{c}}$, $h_{\mathrm{f}} = 0.44\lambda_{\mathrm{c}}$ and $h_{\mathrm{d}} = 0.43\lambda_{\mathrm{c}}$. The reflector and director are placed at distances $l_{\mathrm{r}} = 0.5\lambda_{\mathrm{c}}$ and $l_{\mathrm{d}} = 0.2\lambda_{\mathrm{c}}$ from the feeder element, respectively. The length of the receiving dipole is $h_{\mathrm{dip}} = 0.51\lambda_{\mathrm{c}}$.

The simulated scattering parameters (reflection and transmission) of the antennas are shown in Fig. 2 for a wide range of frequencies, where we can see that both antennas are well matched at the central frequency. In our study we will particularly observe the band of $BW = 10\,\mathrm{MHz}$ around $f_{\mathrm{c}}$. In order to generate the receiving signal, the forward transmission parameter $s_{21}(f)$, i.e. transfer function between ports 1 and 2, has been recorded for different inclination angles $\theta \in [0°, 75°]$ with a $5°$ step, and at $N$ uniformly spaced frequency points within the band of interest, i.e. the set of sample frequencies is defined by $f_n = f_{\mathrm{c}} - BW/2 + (n-1)BW/(N-1)$, where $n \in \{1, 2, ..., N\}$. This data will allow us to observe how the signal-processing algorithm handles the angle-dependent phase characteristic of the transfer function. In Fig. 3 example phase and group delay characteristics of $s_{21}$ are plotted with respect to frequency. The group delay is derived from the transmission parameter

$$\tau_{\mathrm{gd}}(f) = -\frac{1}{2\pi}\frac{\mathrm{d}}{\mathrm{d}f}\arg\{s_{21}(f)\}. \tag{1}$$

## IV. Signal model and estimation algorithm

The proposed bandpass signal consists of a periodic and orthogonal polyphase sequence of complex numbers, $\mathbf{b} \in \mathbb{C}^{N\times 1}$, $|b_n| = 1$. Such sequences are usually used in spread-spectrum systems [10]. In our examples, the sequence is transmitted in $M$ consecutive frames. At the receiver side, the transmitted frame is altered by the transfer function, which includes impact of antennas and of the propagation path, with addition of white noise. Therefore, the $m$-th frame received by the half-wave dipole, $\mathbf{x}_m \in \mathbb{C}^{N\times 1}$, can be expressed as time-domain (TD) baseband model

$$\mathbf{x}_m = \mathbf{a}\mathrm{e}^{\mathrm{j}\gamma_m} + \mathbf{n}_m,\ m = 1, 2, ..., M, \tag{2}$$

where $\gamma_m$ is the constant corresponding to the initial phase of the $m$-th frame and $\mathbf{n}_m \in \mathbb{C}^{N\times 1}$ is the noise vector. The vector $\mathbf{a}$ is given by

$$\mathbf{a} = (\mathbf{TW})^{\mathrm{H}}(\hat{\mathbf{s}}_{21} \odot \hat{\mathbf{b}}), \tag{3}$$

where $\mathbf{W} \in \mathbb{C}^{N\times N}$ is the discrete Fourier transform (DFT) matrix, $\mathbf{T} \in \mathbb{R}^{N\times N}$ is the permutation matrix (shifts DC component to the center of the spectrum)

$$\mathbf{T} = \begin{bmatrix} \mathbf{0} & \mathbf{I}_{N/2} \\ \mathbf{I}_{N/2} & \mathbf{0} \end{bmatrix}, \tag{4}$$

$\mathbf{I}_{N/2}$ is the identity matrix of size $N/2$, $\hat{\mathbf{b}} = \mathbf{TWb} \in \mathbb{C}^{N\times 1}$ is the frequency-domain (FD) spectrum of the sequence, $\hat{\mathbf{s}}_{21} \in \mathbb{C}^{N\times 1}$ is the column vector containing samples of the parameter $s_{21}(f_n)$ for a particular inclination angle $\theta$ and $d_0$. The hat sign denotes FD magnitudes and $\odot$ represents the Hadamard product.

The comprehensive model of the received signal for an unknown distance $d$ and angle $\theta$ would be

$$\mathbf{y}_m = \mathbf{u_a}\mathrm{e}^{\mathrm{j}\gamma_m} + \mathbf{n}_m, \tag{5}$$

where $\mathbf{u_a} = (\mathbf{TW})^{\mathrm{H}}(\hat{\boldsymbol{\alpha}} \odot \hat{\boldsymbol{\beta}} \odot \hat{\mathbf{b}})$, $\hat{\boldsymbol{\alpha}} \in \mathbb{R}^{N\times 1}$ is the magnitude spectrum of the transfer function and the elements of $\hat{\boldsymbol{\beta}} \in \mathbb{C}^{N\times 1}$ are given by $\hat{\beta}_n = \mathrm{e}^{\mathrm{j}\phi_n}$, where $\phi_n = \phi(f_n)$ is the discrete phase spectrum of the transfer function. Thus, in such a model we have $2N$ unknown parameters. This large estimation problem can be simplified using following approximations: (i) Since the transmitted sequence is known and its magnitude spectrum is flat [10], we can perform magnitude equalization at the receiver and obtain the equalized signal and its respective model for a single frame as

$$\mathbf{x}_m^{\mathrm{eq}} = (\mathbf{TW})^{\mathrm{H}}(\hat{\mathbf{x}}_m \oslash \overline{|\hat{\mathbf{x}}|}) \quad \Rightarrow \quad \mathbf{y}_m^{\mathrm{eq}} = \mathbf{u}_{\mathbf{a}}^{\mathrm{eq}}\mathrm{e}^{\mathrm{j}\gamma_m} + \mathbf{n}_m, \tag{6}$$

where $\overline{|\hat{\mathbf{x}}|} = \frac{1}{M}\sum_{m=1}^{M}|\hat{\mathbf{x}}_m|$ is the mean magnitude spectrum of $\mathbf{x}$, the operator $|\,.\,|$ returns the vector of element-wise absolute values, $\oslash$ is the element-wise division and $\mathbf{u}_{\mathbf{a}}^{\mathrm{eq}} = (\mathbf{TW})^{\mathrm{H}}(\hat{\boldsymbol{\beta}} \odot \hat{\mathbf{b}})$. (ii) Secondly, since the signal model is narrowband, the phase characteristic is approximated by a linear function, and therefore, according to (1), the group delay is approximated by a constant $\tau_{\mathrm{gd}}(f) \approx \tau_{\mathrm{gd}}(f_{\mathrm{c}})$ in proximity of $f_{\mathrm{c}}$. It follows that $\hat{\beta}_n \approx \hat{v}_n(d) = \mathrm{e}^{-\mathrm{j}\frac{2\pi f_n}{c}d}$, where it is assumed that $d \approx c\tau_{\mathrm{gd}}(f_{\mathrm{c}})$. Let us define a grid of distances

$d_k$, $k = 1, 2..., K$, that correspond to different traveling times of the signal. We can now write the signal model for each point on the grid

$$\mathbf{y}_m^{\mathrm{eq}}(d_k) \approx \mathbf{u}(d_k)\mathrm{e}^{\mathrm{j}\gamma_m} + \mathbf{n}_m, \tag{7}$$

where $\mathbf{u}(d_k) = (\mathbf{TW})^{\mathrm{H}}(\hat{\mathbf{v}}(d_k) \odot \hat{\mathbf{b}})$ and

$$\hat{\mathbf{v}}(d_k) = [\mathrm{e}^{-\mathrm{j}\frac{2\pi}{c}d_k f_1}, \mathrm{e}^{-\mathrm{j}\frac{2\pi}{c}d_k f_2}, ..., \mathrm{e}^{-\mathrm{j}\frac{2\pi}{c}d_k f_N}]^{\mathrm{T}} \tag{8}$$

is the *delay manifold* vector. This model is justified by the level of collinearity of vectors $\mathbf{u}$ and *equalized* $\mathbf{a}$ from (3), given as

$$\mathbf{a}^{\mathrm{eq}} = (\mathbf{TW})^{\mathrm{H}}(\hat{\mathbf{v}}_{\mathrm{c}} \odot \hat{\mathbf{b}}), \tag{9}$$

where $\hat{\mathbf{v}}_{\mathrm{c}}(d_k, f_{\mathrm{c}}) = [\mathrm{e}^{-\mathrm{j}\frac{2\pi}{c}d_k f_{\mathrm{c}}}, ..., \mathrm{e}^{-\mathrm{j}\frac{2\pi}{c}d_k f_{\mathrm{c}}}]^{\mathrm{T}}$. The measure of this collinearity is their scalar product $\chi(d, \theta, f_{\mathrm{c}}) = \|\mathbf{u}^{\mathrm{H}}\mathbf{a}^{\mathrm{eq}}\|/(\|\mathbf{u}\|\|\mathbf{a}^{\mathrm{eq}}\|)$. Our simulations show that for the adopted set of parameters $f_{\mathrm{c}}$, $BW$, $\theta$ and $d_0$, the collinearity is as high as $\chi > 0.941$.

The simplified model in (7) is analogous to the signal model used in spatial (angular) domain for sensor arrays, where $\mathbf{u}$ corresponds to the steering vector and $\gamma_m$ to the phase at the reference point of the sensor array. Due to this analogy, the algorithms used for parameter estimation in angular domain, e.g. MUSIC, can be applied in time-frequency domain. In order to apply MUSIC, we define matrix $\mathbf{X} \in \mathbb{C}^{N\times M}$, which is obtained by joining together $M$ signal frames $\mathbf{x}_m^{\mathrm{eq}}$, and the estimation of its covariance matrix, $\mathbf{R_{XX}} = \frac{1}{M}\mathbf{XX}^{\mathrm{H}}$. Finally, for given $\theta$, we can write the MUSIC spectrum as

$$P_{\mathrm{MUSIC}}(d_k) = \frac{\mathbf{u}(d_k)^{\mathrm{H}}\mathbf{u}(d_k)}{\mathbf{u}(d_k)^{\mathrm{H}}\mathbf{Q}_n\mathbf{Q}_n^{\mathrm{H}}\mathbf{u}(d_k)}, \tag{10}$$

where $\mathbf{Q}_n \in \mathbb{C}^{N\times(N-1)}$ is the noise subspace matrix of $\mathbf{R_{XX}}$ [7] and the denominator $\mathbf{u}(d_k)^{\mathrm{H}}\mathbf{u}(d_k)$ represents a scaling factor. The estimation of electrical distance between antennas is obtained by

$$\tilde{d}(\theta, f_{\mathrm{c}}) = \max_{d_k}\{|P_{\mathrm{MUSIC}}(d_k)|\}. \tag{11}$$

## V. Numerical examples

Besides the data acquired from the simulated scenario in Fig. 1, in order to test the algorithm, we define here further parameters of our experiment. We use sequences of different lengths, $N \in \{16, 64, 256\}$. Such sequence is repeated $M = 100$ times. For each inclination angle $\theta$ we perform 100 estimations of distance $d$, while the signal-to-noise ratio is set to $SNR = 30\,\mathrm{dB}$. In this study, such relatively high $SNR$ level is chosen in order to distinguish the imperfections of the transmission channel and of the algorithm from the noise effects. The search space (range) for the estimated distance $\hat{d}$ directly affects the size of the problem, i.e. the computation time. However, since the physical distance between antennas is known *a priori*, in this work, a range of only $1\,\mathrm{m}$ is considered in order to assess the accuracy of the proposed algorithm. Therefore, the chosen grid resolution is $\Delta d = 0.1\,\mathrm{mm}$. The results of the MUSIC estimations for $N = 16$, as well as the normalized group delay at the central frequency $c\tau_{\mathrm{gd}}(f_{\mathrm{c}})$, are shown in Fig. 4 with respect to $\theta$. For each inclination angle, a set of estimations is performed, the plot of which are given in dots, whereas their average for the given angle is given in solid line. The root mean square (RMS) of the estimation error with respect to $c\tau_{\mathrm{gd}}(f_{\mathrm{c}})$ vs. inclination angle for different sequence lengths is given in Fig. 5.

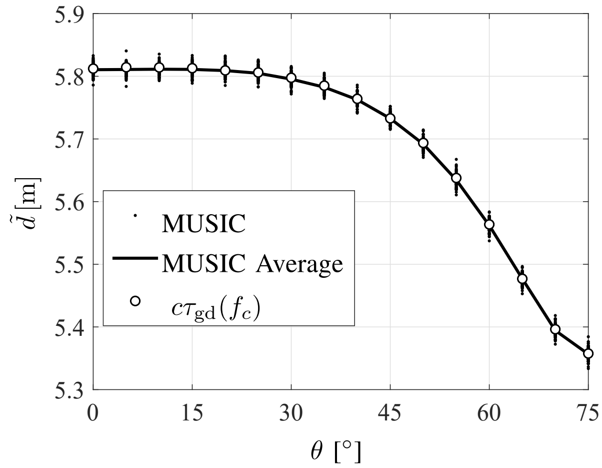


Fig. 4. Estimation of electrical distance between antennas at different inclination angles for $N = 16$. The dots represent single estimations, whereas the solid line is estimated average for each inclination angle. Circles are estimation based on the simulated group delay of the transmission channel.

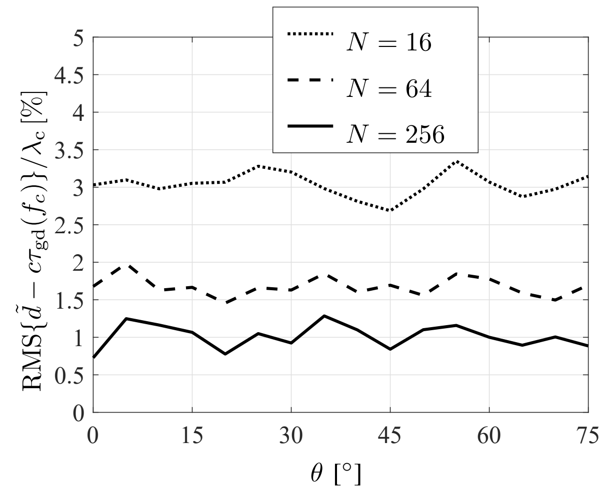


Fig. 5. Normalized root mean square of the estimation error vs. inclination angle for different sequence lengths.

In the first place, we see in Fig. 4 that the estimation obtained through MUSIC algorithm fits very well to the prediction given by the computed group delay, even for a relatively short sequence, when $N = 16$. This verifies the methodology for assessing the algorithm performance, using electromagnetic simulation and proper reference magnitudes. Furthermore, we notice that the relative discrepancy between the simulated physical distance and the normalized group delay is $|d_0 - c\tau_{\mathrm{gd}}(f_c, \theta)|/\lambda_{\mathrm{c}} \in [1.19, 2.71]$. This result might seem surprising, knowing that the maximal diameter of the simulated Yagi-Uda antenna is $0.84\lambda_{\mathrm{c}}$ and that of the dipole is $0.51\lambda_{\mathrm{c}}$. In general, the discrepancy stems largely from the geometrical and electrical properties of the antennas and the environment, which condition the phase characteristic of the total propagation path. The example illustrates effectively the realistic error levels in narrowband ranging applications, in case no calibration of the group-delay bias is available. Finally, in Fig. 5 we observe that the contribution of the algorithm itself to the estimation error is relatively small. Already for $N = 256$, the RMS of the error with respect to $c\tau_{\mathrm{gd}}(f_c)$ approaches $0.75\%$ in terms of $\lambda_{\mathrm{c}}$, which corresponds approximately to $2.25\,\mathrm{mm}$. The results in Fig. 5 show that the accuracy doubles if the length of the sequence is increased four times.

## VI. Conclusion

A method based on a MUSIC-type algorithm for estimation of the electrical distance between two antennas is proposed. The estimation results are compared to the normalized group delay, obtained from the electromagnetic simulation of the scenario. The obtained ranging accuracy increases linearly with the length of the signal sequence and can reach only a fraction of the free-space wavelength. Due to the group-delay variations and simplifications of the signal model, the estimated electrical distance contains a bias error with respect to the physical distance, which can exceed the size of the antennas. This fact is important in distinguishing properties of the estimation algorithm from the inherent physical properties of the transmission channel.

## References


[1] Y. Gu, A. Lo and I. Niemeqeers, A survey of indoor positioning systems for wireless personal networks, in *IEEE Communications Surveys & Tutorials*, vol. 11, 2009, pp. 13-32, 2009.

[2] G. A. Bartels, GPS-Antenna phase center measurements performed in an anechoic chamber, in *Astrodynamics and Satellite Systems*, vol. 8, Delft University Press, 1997.

[3] S. R. Best, Distance-measurement error associated with antenna phase-center displacement in time-reference radio positioning systems, in *IEEE Antennas and Propagation Magazine*, vol. 46, pp. 13-22, 2004.

[4] W. Kunysz, Antenna phase center effects and measurements in GNSS ranging applications, *2010 14th International Symposium on Antenna Technology and Applied Electromagnetics & the American Electromagnetics Conference*, 2010, pp. 1-4, 2010

[5] V. A. Tischenko, V. I. Tokatly and S. A. Kolotygin, The normalized electrical parameters of the antennas of the navigation apparatus of the users of the global satellite navigation systems, in *Measurement Techniques*, vol. 58, pp. 70-74, 2015.

[6] C. Morhart and E. M. Biebl, High resolution time of arrival estimation for a cooperative sensor system, *Adv. Radio Sci.*, vol. 8, pp. 61-66, 2010.

[7] R. Schmidt, Multiple emitter location and signal parameter estimation, in *IEEE Trans. Ant. Prop.*, vol. 34, no. 3, pp. 276-280, 1986.

[8] H. L. Van Trees, *Detection, Estimation, and Modulation Theory Part IV*, John Wiley and Sons, 2002.

[9] http://www.wipl-d.com/products.php?cont=wipl-d-pro.

[10] N. Suehiro and M. Hatori, Modulatable orthogonal sequences and their application to SSMA systems, in *IEEE Transactions on Information Theory*, vol. 34, no. 1, pp. 93-100, 1988.